Cyclic response of reinforced concrete frames partially infilled with relatively weak masonry wall

Mahmoud Baniahmadi [a], Mohammadreza Vafaei [a,*], Sophia C Alih [b]

[a] *School of Civil Engineering, Faculty of Engineering, Universiti Teknologi Malaysia, Skudai, Johor, Malaysia*
[b] *Institute of Noise and Vibration, School of Civil Engineering, Faculty of Engineering, Universiti Teknologi Malaysia, Skudai, Johor, Malaysia*

ARTICLE INFO

ABSTRACT

Partially infilled reinforced concrete (RC) frames have experienced significant damage during past earthquakes. Due to the partial confinement of columns in these structures, the shear force demand increases significantly, resulting in a brittle failure. This study investigated the efficiency of the strong frame-weak infill wall design concept to avoid the brittle failure mode of captive columns. For this purpose, two large-scale partially infilled RC frames with similar material properties and geometry but with different seismic detailing were constructed and subjected to a quasi-static cyclic loading. The obtained results from the conducted experiment were compared with two bare frames with similar detailing and geometry. It was observed that the partially infilled frames had up to 49.6% larger ultimate load than bare frames. Besides, at a 3% drift ratio, the cumulative energy dissipation of partially infilled frames was up to 180% more than bare frames. However, the stiffness degradation rate of the partially infilled frames was higher than the bare frames, particularly at drift ratios less than 1%. Besides, at larger drift ratios (i.e., around 3%), the infill walls contributed to partially infilled frames' lateral strength and increased it up to 60% compared with the bare frames.

1. Introduction

Infill walls play an essential role in the dynamic response of structures when subjected to ground motions. It has been shown during past earthquakes that irregular distribution of infill walls within the plan or height of structures can lead to the partial or complete collapse of buildings [1–3]. On the other hand, infill walls that have been placed symmetrically within the plan and regularly along the height of structures can limit inter-story drifts, enhance the lateral stiffness and strength, and improve the energy dissipation capacity [4–6]. Because of the significant contribution of infill walls in structures' seismic response, many researchers have studied the seismic performance of infilled reinforced concrete (RC) frames. Some studies have focused on the interaction between the infill wall and the surrounding frame considering different parameters like infill wall's material type, aspect ratio, slenderness ratio, and boundary condition [7–10]. Another group of studies has tried to propose macro [11–13] and micro [14,15] models to simulate infill walls' effects during ground motions. Besides, efforts have been made to strengthen masonry-infilled RC frames using different techniques [16] [–] [20].

Partially infilled RC frames have also been studied because of experiencing significant damage during past earthquakes. In many buildings, to provide natural lighting and ventilation, openings are incorporated into the infill walls. In such cases, infill walls often

---

partially confine columns and restrict their ability to deform laterally. When subjected to a lateral force like earthquake forces, the partial confinement increases the shear force demand and results in a brittle failure. As shown in Fig. 1, during past earthquakes, the shear failure of captive columns (i.e. columns that have been partially confined) has been widely reported in several countries [2, 21–25].

Niyompanitpattana and Warnitchai [26] investigated the cyclic response of a long-span partially infilled RC frame designed for gravity loads. They reported that the half-infilled frame's hysteretic behavior was similar to a bare frame up to the drift ratio of 1.5%. However, the partially infilled frame exhibited a significantly larger strength degradation rate and pinching in its hysteresis loops at higher drift ratios. Besides, the measured principal strains on the infill wall did not clearly show the formation of an inclined compression strut. They also stated that the investigated infill wall's behavior could not be simulated by the diagonal strut models that make use of a reduction factor to include the effect of openings. In another study, Pradhan et al. [27] investigated the effects of infill walls aspect ratio and opening size on RC frames' lateral stiffness numerically. They showed that infill walls had an insignificant effect on frames' lateral stiffness when the opening size was larger than 70%. Besides, partially infilled frames with different masonry Young's modulus exhibited similar stiffness degradation patterns. They also found that the shear force in the RC frames' columns was maximum when the height of the infill wall was around 50–60% of the frame's height.

Han and Lee [28] investigated the cyclic response of gravity load-designed partially infilled RC frames. They reported that the longitudinal reinforcements of columns reached yield stress after the shear failure occurred in columns. Besides, the half-infilled RC frame's lateral stiffness was close to that of a bare frame up to the drift ratio of 0.2%. At larger drift ratios, the partially infilled frame's normalized stiffness was less than that of the bare frame. It was also observed that, at the failure load, the energy dissipation of the partially infilled frame was 8% less than the bare frame. The deformation capacity of the partially infilled frame was as low as 80% of the bare frame.

Due to their brittle failure mode, the shear strengthening of captive columns has been the topic of research during past decades. For instance, Jayaguru and Subramanian [29] subjected a two-story two-bay 1/3- scaled partially infilled RC frame to quasi-static cyclic loading and compared its results with a similar structure that was retrofitted by glass fiber reinforced plastic (GFRP). They reported that the ultimate load and stiffness degradation rate of GFRP retrofitted specimen were significantly enhanced. However, the displacement ductility of the GFRP retrofitted specimen was less than half of the un-retrofitted specimen. In another attempt to improve the seismic response of partially infilled frames, Pineda [30] suggested inserting a masonry wall with a horizontal length of twice the opening height at both sides of the vulnerable columns. They stated that the inserted walls could allow for the formation of the compressive strut, which diverted away the large shear force demand from the captive columns. The use of closely spaced transverse reinforcements for the shear strengthening of captive columns has also been investigated. Woodward and Jirsa [31] showed that the shear capacity of a captive column was mainly dependent on the shear capacity of concrete, and transverse reinforcement spacing had an insignificant effect on the shear capacity. Furthermore, the experiments conducted by Maruyama et al. [32] also showed that, at large deformations, an increase in the axial force decreased the effectiveness of transverse reinforcement in maintaining the shear capacity.

In this study, the concept of strong frame-weak infill was investigated for partially infilled RC frames to avoid the shear failure of captive columns and enhance their strength, stiffness, and energy dissipation capacity. This concept has been already examined by few researchers for fully infilled RC frames. For examples, Huang et al. [33] showed that when a strong frame bounds a weak infill wall, a two-line defense system was formed. Such a defense system exhibited an improved seismic response, and the damage to its structural elements could be retrofitted easier. The strong frame-weak infill design concept was also investigated by Dautaj et al. [34]. Based on the conducted tests on eight fully infilled RC frames, they suggested that the strength of RC frames should be at least 1.2 times larger than infill walls for a controlled failure mechanism. On the other hand, the conducted tests on ten single-story fully infilled RC frames showed that strong frame-weak infill structures' cyclic response was favorable irrespective of infill walls' strength and type [35].

In this study, the two RC frames with different seismic detailing but with similar geometry and material properties were constructed and partially infilled with a relatively weak masonry wall. The obtained results from their quasi-static cyclic tests were compared with two bare RC frames that had the same geometry, material properties, and seismic detailing. The subsequent sections describe the test

Fig. 1. Shear failure of a captive column during 2015 Sabah earthquake, Malaysia [2].

specimens and the obtained results for the conducted tests.

2. Test specimens

In this study, two single-story one-bay partially infilled RC frames referred to as PIOF and PISP (see Fig. 2) were constructed and subjected to a quasi-static cyclic loading. The PIOF stands for the partially infilled ordinary moment frame, while the PISF stands for the partially infilled special moment frame. The opening height in both frames is 50 cm. Such an opening is often used for ventilation and lighting of restrooms, storerooms, and school classrooms [36]. These two frames' results were compared with two bare frames referred to as OBF (bare ordinary moment frame) and SBF (bare special moment frame). The OBE and SBF had been tested in another project, and their detailed results can be found in Ref. [37]. It should be mentioned that the material properties, reinforcement ratios, and the sizes of beams and columns in all four RC frames were similar; however, their reinforcement detailing was different. Therefore, following the ACI 318 [38] seismic detailing requirements and classifications, the constructed RC frames were categorized into ordinary (i.e., OBF and PIOF) and special moment frames (i.e., SBF and PISF).

As can be seen from Fig. 3, the lap splice length of reinforcing bars in the columns of ordinary moment frames (i.e., 45 cm) was shorter than seismic codes' requirement (i.e., 74 cm as per ACI 318 [38]). Moreover, their lap splices were located at the base of columns which is not recommended for high ductile RC frames [38]. In ordinary moment frames, the transverse reinforcement spacing at both ends of columns (i.e., 10 cm) and both ends of frame's beam (i.e., 11 cm) was larger than seismic codes' requirement for a high ductile frame [38] (i.e., one-fourth of the effective depth of beams (5.5. cm) and one-fourth of minimum column dimension (5 cm)). Besides, ordinary moment frames did not have any shear link within their beam-to-column joints. However, similar to the special moment frames, they satisfied the requirements of the strong column–weak beam design concept (i.e., the ratio of the sum of nominal flexural strengths of columns ($\sum M_c$) to the sum of nominal flexural strengths of the beams ($\sum M_b$) was 1.4 which was larger than the requirement of ACI 318 (i.e., 1.2) Eurocode 8 [39] (i.e., 1.3)). As can be seen from Fig. 3, unlike the requirement of ACI 318 for high ductile RC frames, the transverse reinforcements of columns in ordinary moment frames did not continue within the frames'
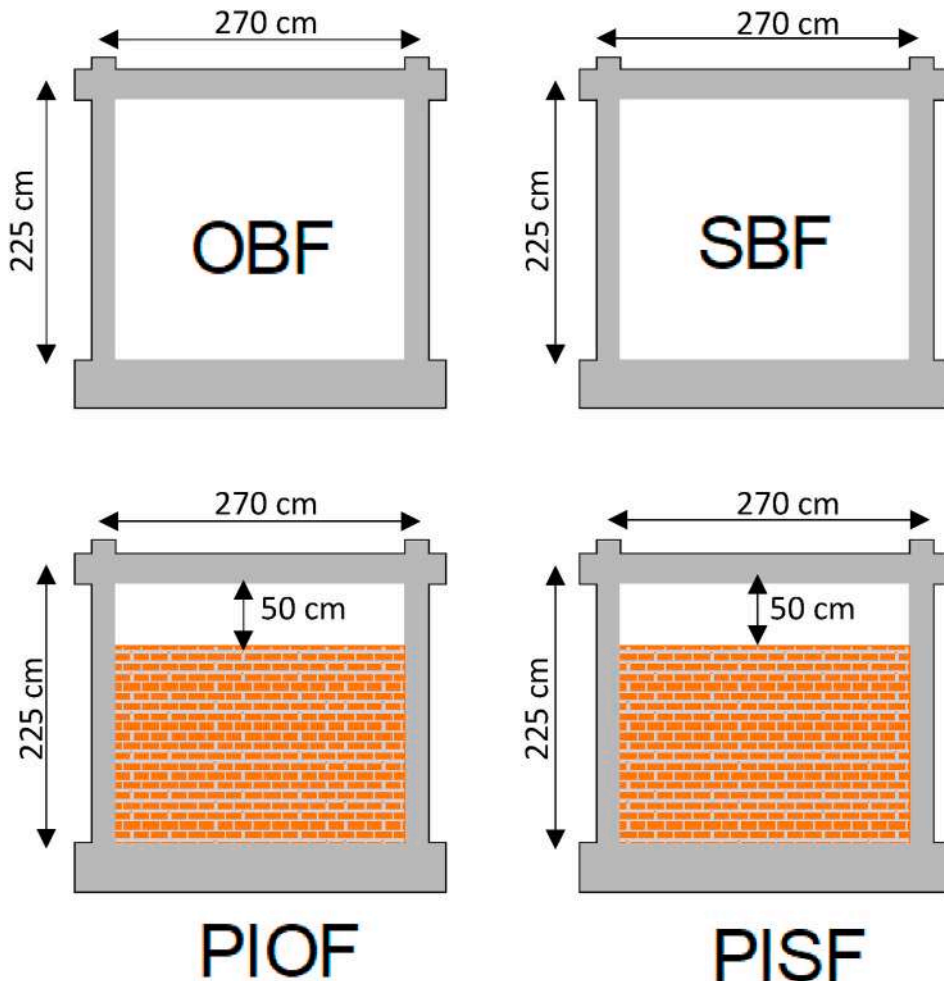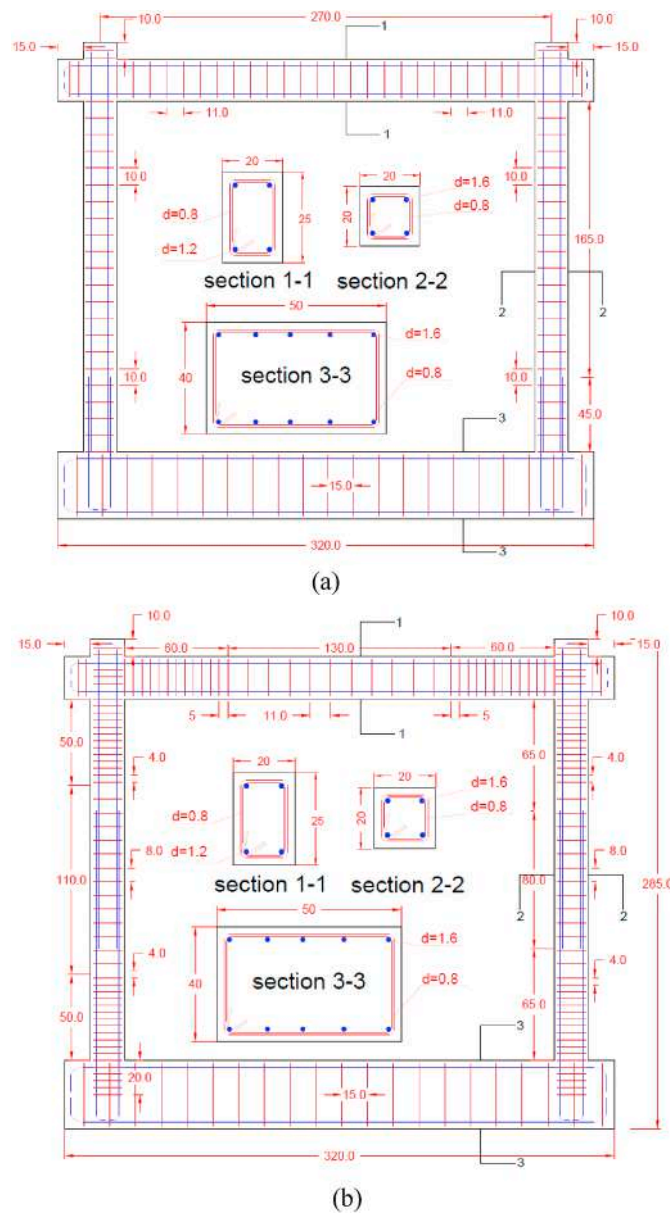

Fig. 2. Tested structures.

Fig. 3. Details of tested specimens (a) ordinary moment frames (b) special moment frames (all dimensions are in cm) [37].

foundation.

As shown in Table 1, the special moment frames satisfied the seismic detailing of high ductile RC frames as per the requirements of ACI 318 [38]. It should be mentioned that all frames had a similar strip foundation that was designed to remain elastic under the applied loads. It is also noteworthy that the reinforcement ratios in columns (i.e., 2%) and beams (i.e., 0.51%) of all frames were within the given range for minimum reinforcement ratio (i.e., 1% of gross-section area for columns and 0.31% for beams reinforced with bars that have the yield stress of 444 MPa) and maximum reinforcement ratio (i.e., 4.5% of gross-section area for columns and 2.5% for beams) [38].

Table 1
Compliance of frames' seismic detailing to the requirements of ACI 318 for a special moment frame [37].

Frame Type	strong column-weak beam	closely spaced hoops in columns	closely spaced hoops in beams	shear reinforcement in joints	adequate length of lap splice	appropriate location for overlapping
ordinary	+	–	–	–	–	–
special	+	+	+	+	+	+

Similar material properties were used to construct the infill walls of PIOF and PISF. In both frames, clay bricks with a thickness of 10 cm were employed. Cement mortar was used in the production of masonry walls with the volume proportion of cement: lime: sand = 1:1:5. The employed mortar had a compressive strength of 5 MPa. The brick masonry walls of PIOF and PISF were constructed similarly 28 days after casting their RC frames. Besides, they were cured three weeks before subjecting them to the imposed loads. The masonry walls' compressive strength was calculated based on the procedure explained in ASTM C1314-16 [40] and equaled 3.9 MPa. The diagonal tension (shear) strength of the brick masonry wall was estimated through conducting experiments on three square samples with the size of 60 cm following the procedure explained in ASTM E519/E519 M − 15 [41]. The average shear strength of the three samples equaled 0.15 MPa. The average compressive strength of concrete based on the conducted tests on standard cylinder specimens was 30 MPa. The average material properties of reinforcing bars based on the conducted tests on three samples have been provided in Table 2.

3. Test setup and instrumentation

As can be seen from Fig. 4, the constructed frames were fixed within a strong steel frame by connecting their foundation to a strong floor. Two hydraulic jacks were installed at both sides of frames for lateral loading of frames at the beam's mid-height. Besides, two load cells (i.e., LC3 and LC4) measured the applied lateral loads to the frames. A constant vertical load of 100 kN was applied to each frame's columns through two high-strength post-tensioned bars. Two load cells (i.e., LC1 and LC2) monitored the intensity of vertical loads. The lateral displacements of frames were measured by Linear Variable Differential Transformers (LVDTs) at the mid-height of frames' beam (see LVDT1 and LVDT2).

As can be seen from Fig. 5, the strain in the longitudinal reinforcements of columns was measured at their base (i.e., ST1), 50 cm below the bottom of the beam (i.e., ST2) and at the top of columns (i.e., ST3). The strain in the top layer of the beam's longitudinal reinforcements was measured at the left end side (see ST4 in Fig. 5). The strain in the stirrup of columns was measured at the level where the infill wall ended (see ST5 in Fig. 5). As can be seen from Fig. 6, the frames were subjected to a quasi-static cyclic load that followed the recommendations of FEMA 461 [42]. The loading history consisted of repeated cycles of step-wise increasing deformation amplitudes. According to FEMA 461 [42], the number of steps in the loading history should be ten or more, and two cycles at each step should be completed. Besides, the amplitude a_{i+1} of the step i+1 is calculated by $a_{i+1} = 1.4b_i$, where b_i is the amplitude of the preceding step.

4. Results and discussions

4.1. Crack patterns and failure modes

a) OBF and SBF specimens

The observed damage to OBF and SBF specimens is shown in Fig. 7. The first crack in both bare frames occurred at the drift ratio of 0.28%. The first crack in SBF was a narrow diagonal crack located at the left beam-to-column joint. However, the first crack in OBF appeared simultaneously at the left end of the beam, left joint, and both ends of the left column. In OBF, concrete spalling was observed at the left column base when the drift ratio reached 1%. However, the concrete spalling in SBF occurred at the drift ratio of 1.5%. Unlike OBF, the observed cracks on the beam of SBF were longer and deeper than cracks observed at the base of columns. Besides, the number of observed cracks on the beam and columns of SBF were relatively less than that of OBF (see Fig. 8), mainly because of the closely spaced stirrups that provided better confinement for the concrete.

As can be seen from Fig. 9, the strain in the longitudinal bar of OBF's beam (see ST4) passed the yield strain when the drift ratio was around 2.7%. The measured strains in the column's longitudinal bar (i.e., ST1, ST2, and ST3) and the shear link (i.e., ST5) of OBF were all below the yield strain. The inadequate lap splice length at the base of OBF's columns was the main reason for the low strains. It should be mentioned that the inadequate lap splice length increased the bond stresses between the concrete and the reinforcing bars and resulted in some vertical cracks at the base of OBF's columns.

As can be seen from Fig. 9, the longitudinal bars in SBF's beam yielded at the drift ratio of 2.1% (a smaller drift ratio compared with OBF). Besides, similar to OBF, the measured strains at the top of the longitudinal bars of SBF's columns (i.e., ST2 and ST3) were below the yield strain. However, at the base of its columns, the longitudinal bars passed the yield strain when the drift ratio reached 3.5%. It is noteworthy that, in SBF, the longitudinal bars of the beam yielded before the longitudinal bars of the column that was mainly because of the employed strong column-weak beam design concept.

b) PIOF and PISF specimen

Since the shear strength of tested specimens' columns was larger than the lateral strength of brick walls, no shear failure was observed in the columns of PIOF and PISF. The shear strength of columns (V_u) was estimated by ASCE 41 [43] equation as shown

Table 2
Material properties of reinforcing bars [37].

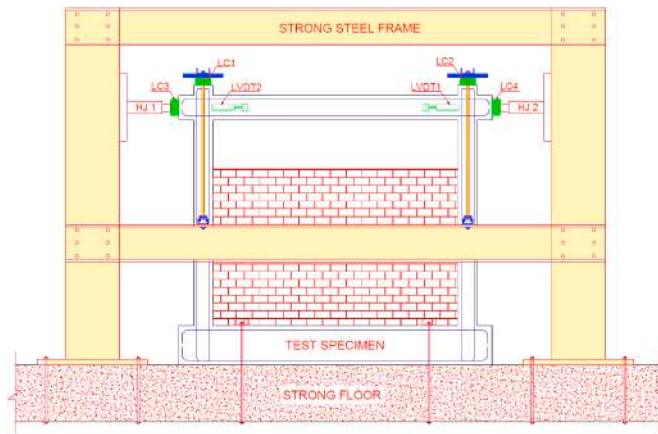| Diameter (mm)	Yield stress (MPa)	Ultimate stress (MPa)	Yield strain (mm/mm)	Ultimate strain (mm/mm)
8	532	693	0.0026	0.086
12	444	565	0.0022	0.112
16	537	681	0.0027	0.092

Fig. 4. The employed test set up.
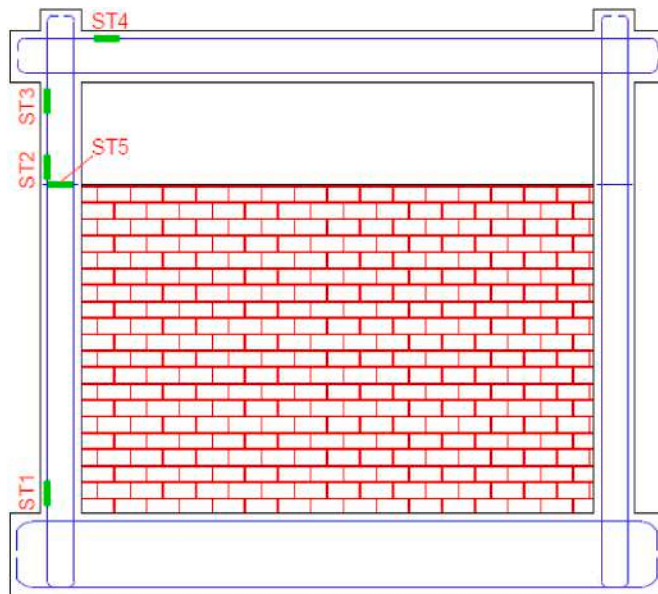

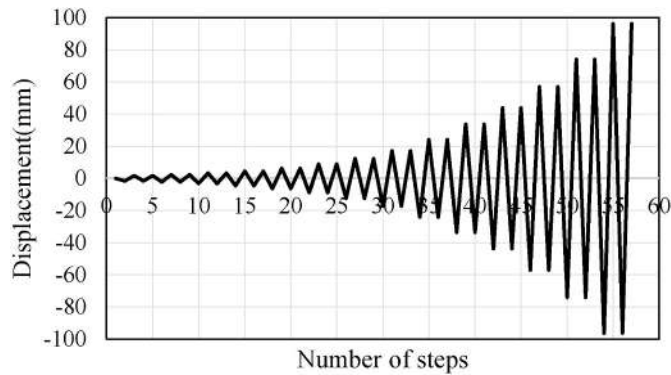**Fig. 5.** Location of strain gauges.
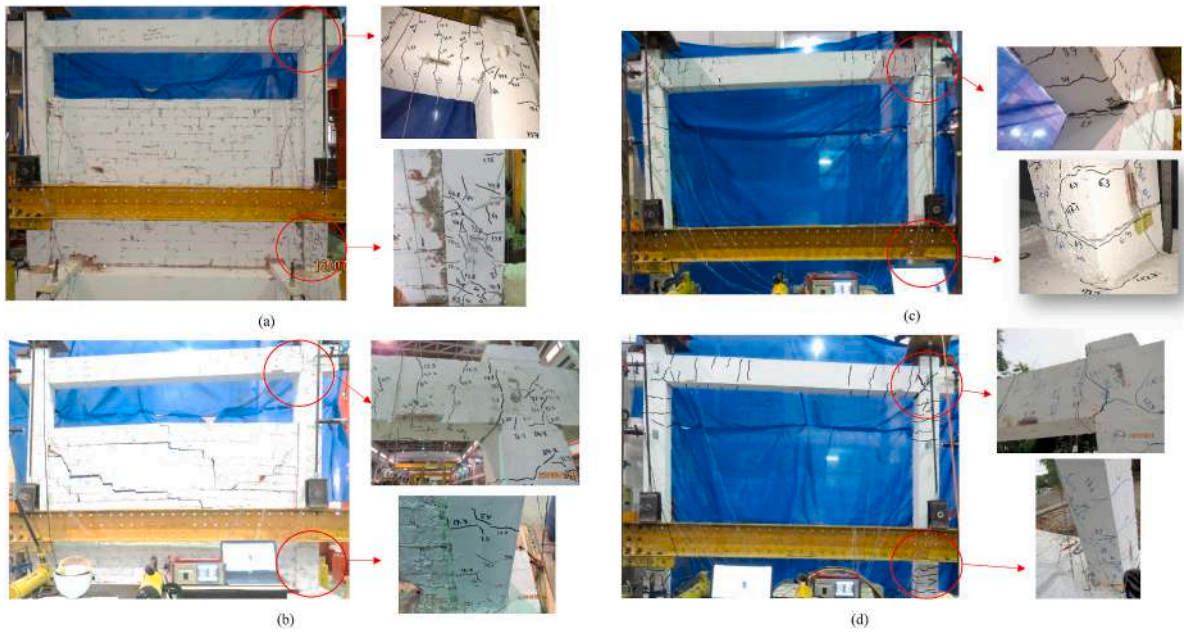

Fig. 6. Employed load protocol.

Fig. 7. Observed damage to partially infilled frames (a) PIOF (b) PISF (c) OBF (d) SBF.
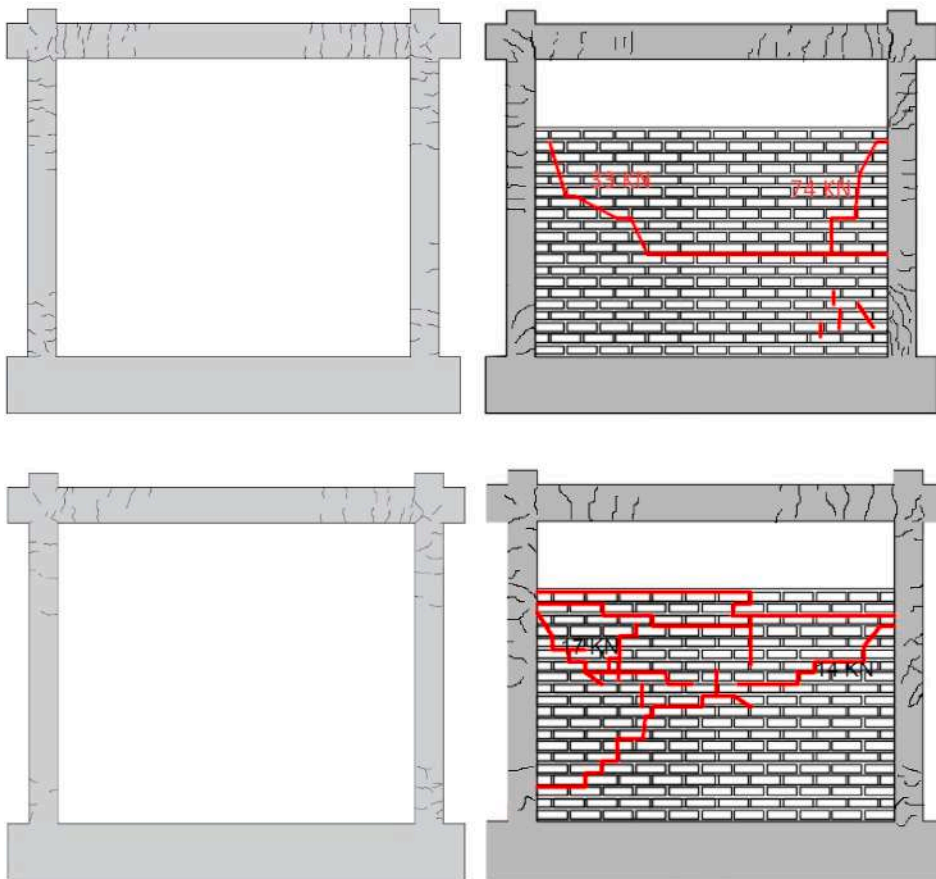

Fig. 8. Crack patterns of test specimens (a) OBF (b) PIOF (c) SBF (d) PISF.
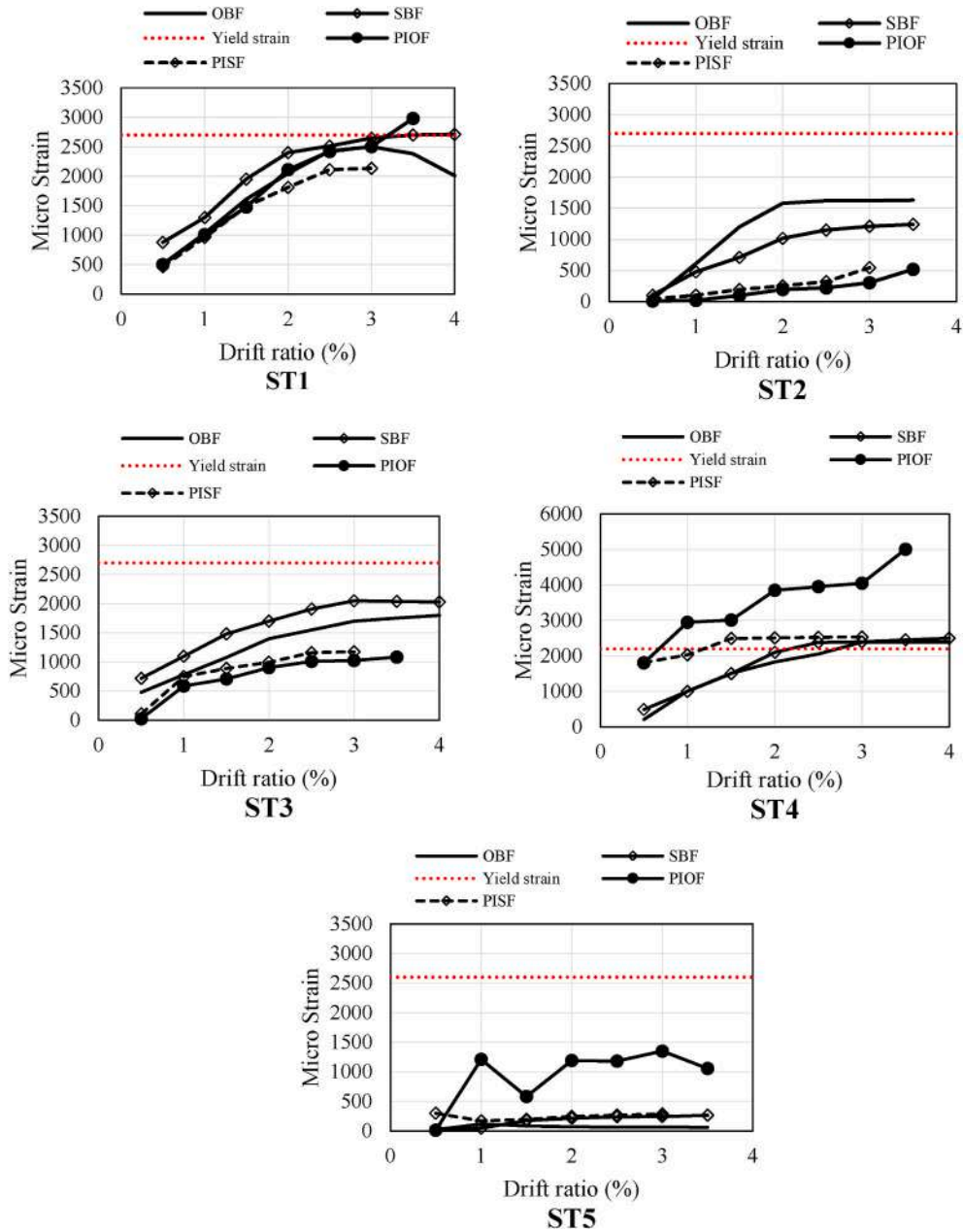
Fig. 9. Measured strains in longitudinal bars and shear links.

below:

$$V_u = \frac{A_{st} f_{yt}\, d}{s} + \left(\frac{0.5\, \sqrt{f_c}}{\frac{a}{d}} \sqrt{1 + \frac{F}{0.5\sqrt{f_{cc}}\, A_g}} \right) 0.8 A_g \tag{1}$$

where, A_{st} and f_{yt} are, respectively, transverse reinforcement area (mm^2) and the yield strength (MPa), f_c is the compressive strength of concrete (MPa), a is the shear span length (mm), d is the effective depth of the column (mm), F is the axial force in the column (N), and A_g is the column's gross cross-sectional area (mm^2). For columns with an ordinary detailing (i.e., columns of OBF and PIOF) =100 mm and $V_u = 132$ kN. This shear strength is almost 20% larger than the maximum lateral force applied to the tested specimens (i.e., 108.2 kN, see Fig. 10).

The infill wall of PIOF exhibited no visible crack until the drift ratio of 0.39%. At this point, the brick wall was separated from the frame's columns. A diagonal crack occurred at the top left corner of the wall when the drift ratio reached 1.55%. The brick wall was
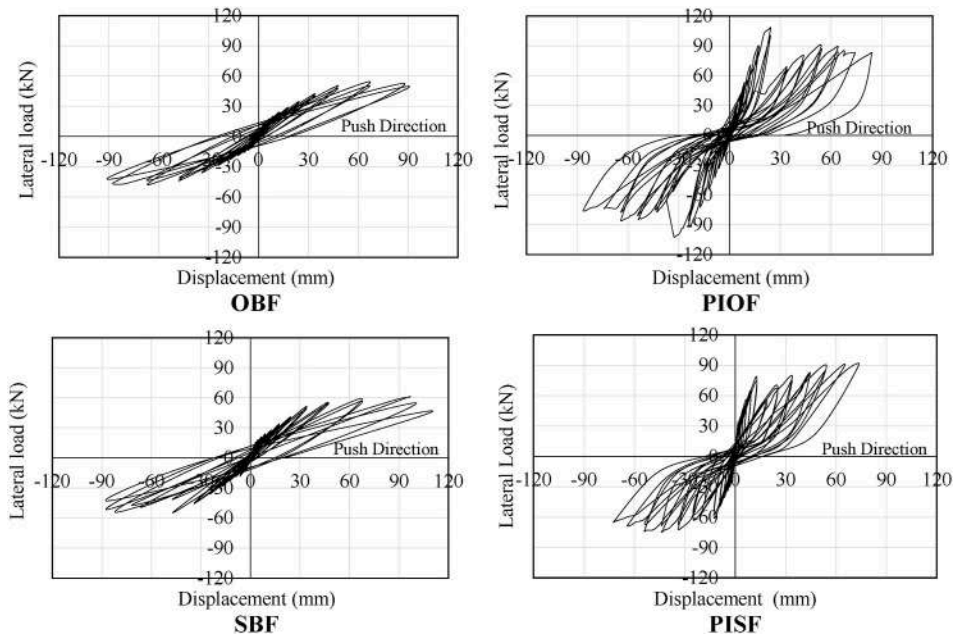
Fig. 10. Hysteresis loops of tested specimens.

crushed at its left corner when the drift ratio was 1.97%. Few bricks were also crushed at the mid-height of the wall when the drift ratio reached 3.3%. At the end of the test, cracks were mostly concentrated at the brick wall's upper mid-height. The bottom part of the wall had only a few short cracks that were close to the bottom of the right column (see Fig. 8). The first crack in the RC frame of PIOF occurred at the left side of its beam when the drift ratio was 0.19%. A crack was observed at the left beam-to-column joint when the drift ratio reached 0.28%. At the same d s rift ratio, a crack was also observed on the right column. The cracks in the beam and columns were flexural type while joints' cracks were shear type. The frame's right column exhibited a narrow diagonal crack, almost 50 cm below the beam's bottom, when the drift ratio reached 1.1%. Concrete spalling was also observed at the base of both columns at the drift ratio of 3.3%.

In PISF, the brick wall was separated from the frame's columns at a drift ratio of 0.4%. The first crack in the wall was observed at the drift ratio of 0.55%. At this drift ratio, the last layer of bricks was partially detached from the mortar. Soon after, the cement mortar laid on top of the last layer of bricks was also detached, and a horizontal crack was observed (see Fig. 8d). Then, at the drift ratio of 0.64%, diagonal cracks appeared in the wall's left and right corners. Stair-stepped shear cracks were first observed at the upper side of the infill wall when the drift ratio reached 0.76%. They were also developed at the mid-height of the infill wall at a drift ratio of 1.9%. The first crack in the RC frame of PISF was observed at the left beam-to-column joint when the drift ratio was 0.1%. Flexural type cracks appeared on its beam at the drift ratio of 0.15%.

In the previous studies conducted on RC frames partially infilled with strong walls, the first crack in the wall has been observed at the drift ratios of 0.6% for a square frame [28] and almost 0.75% for a long-span frame [26]. Therefore, the weak infill wall used in this study has slightly reduced the drift ratio corresponding to the first crack compared with RC frames partially infilled with strong walls. It should be mentioned that RC frames fully infilled with weak masonry walls have shown even a smaller drift ratio corresponding to the first crack of the infill wall. For these structures, the first crack in the weak infill wall has been reported at the drift ratio ranging from 0.06% to 0.14% [33,35].

The presence of infill walls in PIOF and PISF significantly increased the strain in their beams' longitudinal bars (see ST4 in Fig. 9) compared with OBF and SBF specimens. The strain in the beams of PIOF and PISF passed the yield strain, respectively, at the drift ratios of 0.7% and 1.2%. This implied that the infill walls in PIOF and PISF accelerated the yielding of beams' longitudinal bars compared to OBF and SBF specimens. It is also noteworthy that the measured strains at the top of PIOF and PISF's columns (see ST2 and ST3 in Fig. 9) are less than that of bare frames which is similar to what has been reported for RC frames partially infilled with strong infill walls [26,28]. This observation can be attributed to the restraining effect of infill walls. The measured strains at the base of PISF's columns (see ST1) are also less than that of SBF. However, no significant change was found in the measured strain at the base of PIOF's columns up to a drift ratio of 3%. At the drift ratio of 3.2%, the strain in its longitudinal bars passed the yield strain. It is also evident from Fig. 9 that the measured strains in the shear links of all tested specimens are below the yield strain. This indicated that partially infilled brick walls' lateral strength was less than the shear strength of columns. Therefore, as explained earlier, no shear failure occurred in the columns of tested specimens.

A comparison between the crack patterns of bare and partially infilled frames shows that due to infill walls, the number of cracks at the mid-height of columns has increased. A similar observation has been made by other researchers for RC frames partially infilled with strong infill walls [26,28]. This implies that the closely spaced stirrups should be used throughout the length of columns. Besides, it is

evident from Fig. 9 that frames with special seismic detailing (i.e., PISF and SBF) have relatively fewer cracks compared with the frames with ordinary detailing (i.e., PIOF and OBF). The presence of diagonal cracks in the infill wall of PIOF and PISF specimens indicates the inclined compression struts' formation during the cyclic loading. It is worth mentioning that the formation of inclined compression struts was not observed in an experiment conducted on a half-height infilled RC frame [26].

It should also be mentioned that PIOF and PISF specimens were constructed from the same materials, cured under the same condition, and subjected to a similar loading protocol. However, as explained earlier, their infill wall exhibited two different failure mechanisms, and their frames had different strain distributions. Although the observed differences can be related to the employed seismic detailing, a slight difference in their workmanship (i.e., the contact area between columns and bricks, the arrangement of bricks within the wall, thickness of mortar, etc.) might have also contributed to the differences observed in their response.

(Note: ST1, ST, and ST3 show the measured strains in the longitudinal bar of the left column at the base, below the opening, and top of the column, ST4 shows the measured strain in the reinforcing bar of the beam at its left corner, and ST5 shows the strain in the stirrup of the left column measured below the opening level).

4.2. Hysteresis loops

The tested specimens' hysteresis loops are shown in Fig. 10, and their backbone curves are plotted in Fig. 11. It is evident from these two figures the partially infilled frames have larger ultimate loads compared with the bare frames. In the push direction, the ultimate load of PIOF is 108.2 kN which is 49.6% larger than that of OBF (i.e., 54.5 kN). The ultimate load of PISF is 90 kN which is 31.7% larger than that of SBF (i.e., 61.5 kN). The increase in the ultimate loads of PIOF and PISF compared with bare frames is because of their infill walls' contribution to the lateral response as observed by other researchers [26,28]. It should be mentioned that RC frames partially infilled with strong walls have shown up to a 10.8% increase in the ultimate strength compared with a bare frame which is significantly less than the obtained results in this study [26,28]. The main reason is the shear failure of columns which occurs when the strength of the infill wall is more than the shear capacity of columns. It is worth mentioning that the increase in the ultimate loads of RC frames fully infilled with a weak infill wall compared with a bare frame has been in the range of 20–25% [33,35].

In the pull direction, the ultimate loads of tested specimens are less than that of the push direction. The ultimate loads of PISF, PIOF, SBF, and OBF show, respectively, 17%, 5.4%, 11.5%, and 11.7% decrease compared with the push direction. This observation is mainly because of cracks that occur in the infill wall, beam, and columns of test specimens when they are loaded in the push direction and has also been reported by other researchers [28]. It is noteworthy that, although the ultimate load of SBF is 11.4% more than OBF, the ultimate load of PISF is 37.5% less than that of PIOF. The reason for this observation relies on the fact that the infill walls of PIOF and PISF exhibited two different failure mechanisms (see Fig. 8). Therefore, despite having similar material properties and geometry, their contribution to the lateral strengths of PIOF and PISF has not been similar.

As can be seen from Fig. 11, both PISF and PIOF experience a sudden drop in their lateral strength at two different drift ratios of 0.76% and 1.5%, respectively. At these drift ratios, the stair-stepped shear cracks appeared in the brick wall of PISF, and diagonal cracks were observed in the infill wall of PIOF. It is also noteworthy that the lateral strength of both frames keeps increasing after the first drop. However, in PIOF, the lateral strength remains below the measured strength at the first peak, while in PISF, it passes the first peak in the strength. It can also be seen that, at large drift ratios, the lateral strength of PIOF approaches to that of PISF. This indicates that the infill wall of PIOF has a higher strength degradation rate compared with that of PISF. It should be noted that, at large drift ratios, the lateral strengths of the partially infilled frames are greater than the bare frames. Therefore, even at large drift ratios (i.e., >3%), the infill walls have contributed to the lateral strengths of PIOF and PISF. It is worth mentioning that, in previous studies, the contribution of infill wall to the lateral strength of RC frames has been reported up to the drift ratios of 1% (for a fully infilled RC frame) [35], 1.7% (for a half-height partially infilled and lightly reinforced RC frame) [28], and 2% (for a long span half-height partially
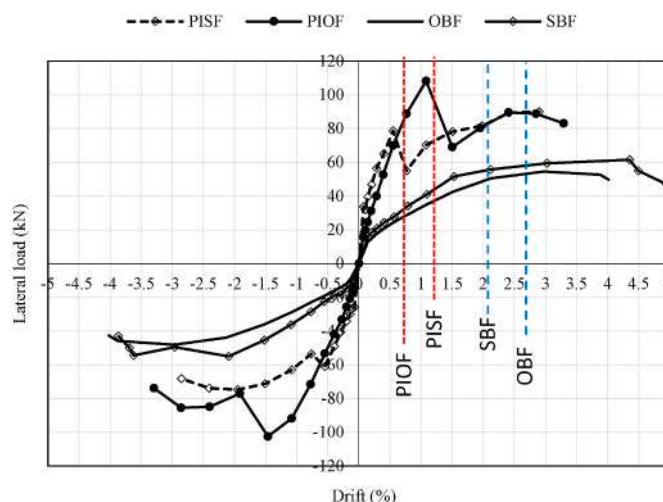

Fig. 11. Backbone curves of tested specimens (the dashed lines show the drifts corresponding to the yielding of beam's reinforcing bars).

infilled RC frame) [26].

The drift ratios in which the beam's reinforcing bar has reached the yield strain are shown in Fig. 11 by vertical dashed lines. As can be seen, in PIOF, the beam's reinforcing bar reach the yield strain before the infill wall reach its ultimate strength (i.e., the first peak in the response curve). This implies that, unlike the general belief in earthquake engineering [14], the RC frame in PIOF has acted as the first line of defense against the lateral loads. It is worth mentioning that the obtained results from this study correlate well with the findings of other researchers that examined the seismic performance of low ductile RC frames infilled with low-strength masonry walls [44]. It should be mentioned that, in PISF, the yielding of the beam's reinforcing bar occurs after the first peak in the strength of the frame-infill system (i.e., after the occurrence of stair-stepped shear cracks in the brick wall). Therefore, unlike PIOF, the brick wall has acted as the first defense line. This observation is mainly due to the failure mechanism of infill wall and the higher ductility of RC frame in PISF.

OBF and SBF reach their ultimate strength in the push direction at the drift ratios of 2.97% and 4.3%, respectively. However, PIOF and PISF reach their ultimate strength at the drift ratios of 1.1% and 2.89%, respectively. Therefore, the presence of infill walls in PIOF and PISF has reduced the drift ratios that correspond to the ultimate loads by 62.9% and 32.8%, respectively. Besides, in the push direction, the drift ratio corresponding to the ultimate load of PISF is 63.9% larger than that of PIOF. This indicates that the employed special seismic detailing in PISF and SBF has enhanced their deformation capacity compared with PIOF and OBF.

Considering the observed stair-stepped shear cracks in the brick wall of PISF, the widely employed single-strut macro-models [14] may not accurately estimate the lateral strength of partially infilled RC frames. Therefore, for the numerical simulation of partially infilled RC frames, a preliminary study based on the proposed failure theories [45,46] should be conducted, and the governing failure modes of the brick walls should be identified. When stair-stepped shear cracks dominate the infill wall's failure mode, macro-models that consider the shear failure along mortar joints or the diagonal tension failure [47] may be used.

4.3. Displacement ductility ratios

The displacement ductility ratio (μ) of test specimens was defined as the ratio of displacement at the ultimate load to the displacement at the effective yield point. The displacement at the effective yield point was calculated through the bilinear representation of backbone curves using the recommended procedure in FEMA 356 [48]. As can be seen from Fig. 12, the bilinear representation of the backbone curve follows the equal energy approach (i.e., the area under the backbone curve equals the area under the bilinear representation). In Fig. 12, F_y and Δ_y are the strength and displacement at the effective yield point, respectively. It should be mentioned that the first segment of the bilinear representation intersects with the backbone curve at $0.6F_y$. The first segment's slope is called the effective stiffness, and that of the second segment is referred to as the post-yield stiffness.

Tables 3 and 4 summarize the calculated parameters based on the bilinear representation of backbone curves for push and pull directions, respectively. As can be seen from these tables, infilled frames have larger effective yield strengths when compared with the bare frames. It is also seen that the effective yield strengths of SBF are larger than OBF. However, the effective yield strengths of PISF are smaller than PIOF. These observations imply that the partially infilled frames' effective yield strengths have been controlled by the failure mechanism of their infill wall rather than the ductility of their RC frame.

The obtained results also show that the effective yield displacement of SBF is larger than OBF. However, the effective yield displacement of PISF is significantly less than PIOF, mainly because the infill wall of PISF was cracked earlier than PIOF. The calculated displacement ductility ratios (DDRs) indicate that the frames with special seismic detailing (i.e., SBF and PISF) have larger DDRs compared with frames without seismic detailing (i.e., OBF and PIOF). It is noteworthy that the increase in the DDR of PISF compared with PIOF is significantly more than the increase in the DDR of SBF when compared with OBF. Besides, it can be seen that the DDR of PIOF is almost 1/3 of OBF, while the DDR of PISF is almost 2.6 times larger than SBF. In other words, the infill wall presence has decreased the DDR of PIOF and has increased the DDR of PISF compared with bare frames. The main reason for this observation is that the effective yield displacement of OBF is very close to that of PIOF. However, the effective yield displacement of PISF is significantly
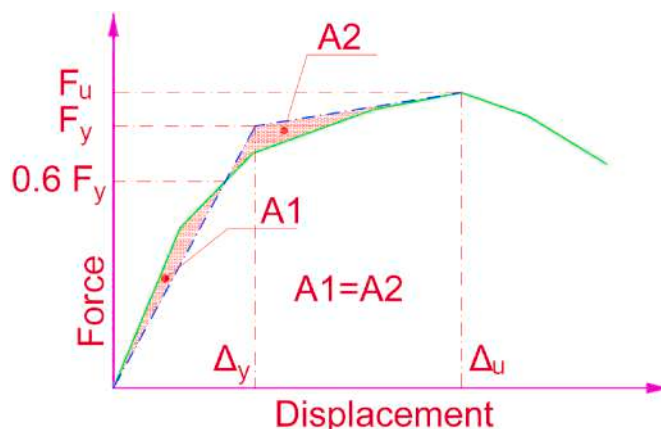

Fig. 12. Bilinear representation of the backbone curve [48].

Table 3
Obtained results from bilinear representation of backbone curves for the push direction.

Frame ID	Effective stiffness (kN/mm)	Post-yield stiffness (kN/mm)	Dis. ductility $\mu = (\frac{\Delta_u}{\Delta_y})$	Displacement (mm)		Strength (kN)	
				Δ_u	Δ_y	F_u	F_y
OBF	2.00	0.34	3.51	66.85	19	54.5	38
SBF	2.20	0.14	4.21	96.8	23	61.5	50.5
PIOF	5.58	0.86	1.31	24.3	18.5	108.2	103.2
PISF	10.85	0.44	11.02	65.02	5.9	90	64.1

Table 4
Obtained results from bilinear representation of backbone curves for the pull direction.

Frame ID	Effective stiffness (kN/mm)	Post-yield stiffness (kN/mm)	Dis. ductility $\mu = (\frac{\Delta_u}{\Delta_y})$	Displacement (mm)		Strength (kN)	
				Δ_u	Δ_y	F_u	F_y
OBF	1.5	0.38	3.03	66.74	22	48.1	33
SBF	1.78	0.15	3.14	81.51	26	54.4	46
PIOF	3.63	0.77	1.47	32.85	22.4	102.4	94.4
PISF	6.51	0.55	5.15	43.83	8.5	74.7	55.4

less than SBF. It should be also mentioned that the deformation capacity of an RC frame partially infilled with a strong infill wall has been as low as 80% of the bare frames [28]. However, an RC frame fully infilled with a weak infill wall has shown around 22.9% larger DDR compared with a bare frame [33].

It can also be seen from Tables 3 and 4 that the infill wall's presence has increased the effective yield stiffness of PIOF and PISF compared with bare frames. Although the effective stiffness of PISF is larger than PIOF, the post-yield stiffness of PIOF is more than PISF. This implies that, compared with PISF, PIOF has a larger reserved strength after passing the effective yield point. Therefore, the partially infilled RC frames' post-yield stiffness has been affected mainly by their infill wall's failure mechanism rather than the ductility of their RC frames.

4.4. Stiffness degradation rate

The initial lateral stiffness (i.e., secant stiffness) of OBF, SBF, PIOF, and PISF in the push direction was, respectively, 4.16, 4.58, 9.7, and 10.1 kN/mm. Therefore, the initial stiffness of partially infilled RC frames was almost twice that of the bare frames. In the previous study on a half-height infilled RC frame, only a 50% increase in the initial stiffness has been reported [28]. In the pull direction, the initial lateral stiffness of OBF, SBF, PIOF, and PISF were reduced to 4.10, 2.73, 8.34, and 8.81 kN/mm, respectively. The reduction in the initial stiffness of test specimens in the pull direction is related to the cracks forming in the columns, beam, and infill wall during the loading in the push direction. The test specimens' lateral stiffness was normalized by the stiffness measured at the beginning of the tests (i.e., initial stiffness). The normalized stiffness degradation curves of tested specimens are shown in Fig. 13. As can be seen, PISF has a higher normalized stiffness degradation rate compared with PIOF. The main reason for this observation is that cracks were developed in the infill wall of PISF earlier than PIOF. It is also seen that, at large drift ratios, the normalized stiffness of PISF and PIOF is less than bare frames. This observation correlates well with the obtained results from previous studies [28,35]. A sharp decrease in the lateral stiffness of PISF and PIOF can be seen around 0.6% and 1.2% drift ratios, respectively, which is because of the development of diagonal cracks in their infill wall. It is noteworthy that even at small drift ratios (i.e., around 0.5%), all tested frames have lost at least 40% of their initial stiffness. This implies that even under medium intensity earthquakes, RC structures' natural period can be significantly increased.

4.5. Energy dissipation

The enclosed area by the force-displacement loops was calculated at each drift ratio to determine test specimens' energy dissipation. Then, the cumulative energy dissipation was obtained by summing up the calculated areas at each drift ratio. The cumulative energy dissipation curves have been presented in Fig. 14. It is evident from this figure that, at very small drift ratios (i.e., less than 0.2%), the tested frames' energy dissipation is close to each other. This is mainly because the tested specimens are in the elastic range when the drift ratio is small; therefore, the share of plastic deformation in the dissipated energy is insignificant. As the drift ratio increases, the partially infilled RC frames' energy dissipation becomes significantly greater than the bare frames. This observation indicates the significant contribution of infill walls to the dissipated energy by PIOF and PISF. It should be mentioned that the energy dissipation capacity of an RC frame partially infilled with a strong wall has been 8% less than a bare frame [28]. Besides, an RC frame fully infilled with a weak wall has shown 7% larger cumulative energy dissipation compared with a bare frame [33].

It is noteworthy that the energy dissipation of PISF is larger than PIOF up to the drift ratio of 1.2%. This observation relies on the fact that the development of cracks in the infill wall of PISF was earlier than PIOF; therefore, the contribution of infill wall in the energy dissipation of PISF has started earlier than PIOF. However, as soon as diagonal cracks were developed in the infill wall of PIOF, its energy dissipation reached the level of PISF (see drift ratio of 1.5%). It is also noteworthy that despite the smaller ultimate strength of PISF compared with PIOF, its energy dissipation at large drift ratios is close to that of PIOF. This observation implies that, at large drift
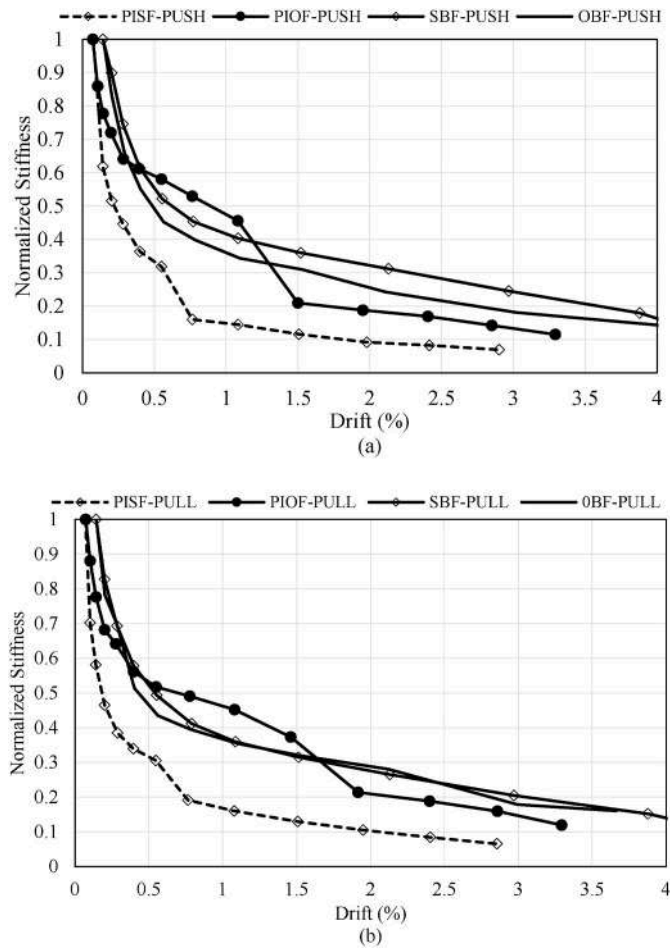
Fig. 13. Normalized stiffness degradation of tested specimens (a) push direction (b) pull direction.

ratios, the infill wall's failure mechanism has an insignificant effect on the partially infilled frames' energy dissipation capacity.

5. Conclusions

This study investigated the cyclic response of partially infilled RC frames. Two RC frames were constructed and infilled with weak masonry brick walls such that no shear failure could occur in columns. The seismic detailing of the constructed RC frames was different. One of the frames (i.e., PISF) followed the special seismic detailing of ACI 318 [38] while the second frame (i.e., PIOF) had an ordinary reinforcement detailing. Both frames had similar geometry and material properties and were subjected to a similar quasi-static cyclic loading. The obtained results from the conducted experiment were compared with two bare frames with the special seismic detailing (i.e., SBF) and an ordinary reinforcement detailing (i.e., OBF). The following conclusions can be derived from this study:

1. The number of cracks in frames with special seismic detailing (i.e., PISF and SBF) was less than frames with ordinary seismic detailing. Besides, the length and depth of observed cracks in PISF and SBF were shorter and shallower. Therefore, frames with special seismic detailing could have relatively lower repair costs.
2. Partially infilled columns exhibited more cracks at the mid-height of their columns when compared with the bare frames. Therefore, for improving their ductility, closely spaced stirrups should be used throughout their length.
3. The presence of infill walls in PIOF and PISF significantly increased the measured strains in their beams' longitudinal bars and decreased the measured strains at the top of their columns when compared with bare frames.
4. In PIOF and PISF, the beam's longitudinal bar yielded at a drift ratio close to 1.0%. However, the yielding of their columns' reinforcing bar (measured at top) was at a drift ratio larger than 3%. Although this is a preferable sequence for reinforcing bars' yielding, under a medium intensity earthquake, the beams of partially infilled frames may require extensive repair. It should be mentioned that, in bare frames, the longitudinal bars reached their yield strain at a drift ratio close to 2.5%.
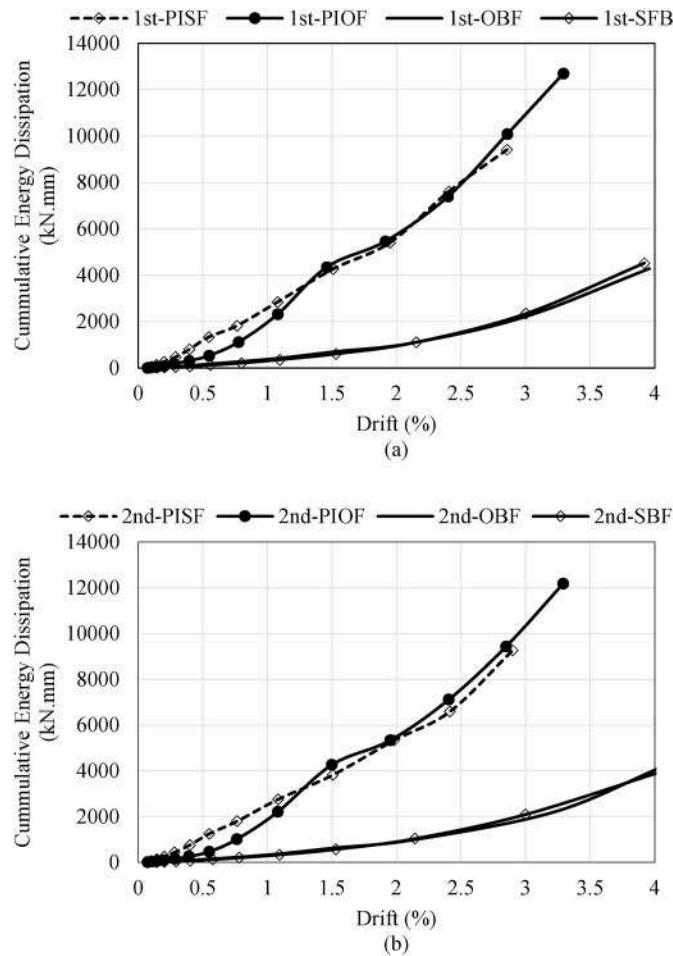
Fig. 14. Cumulative energy dissipation curves (a) first cycle of loading (b) second cycle of loading.

5. Although the ultimate strength of SBF was 12.8% greater than OBF, the ultimate strength of PISF was 20.2% less than PIOF. This indicated that the ultimate load of partially infilled frames was affected mainly by their infill wall's failure mechanism rather than their ductility level (i.e., seismic detailing).

6. The ultimate strengths of partially infilled frames were up to 49.6% larger than the bare frames, even at large drift ratios (i.e., around 3%) they exhibited up to 60% larger lateral strength than bare frames. This implied that infill walls contributed to RC frames' lateral response even after they experienced significant damage. Therefore, under strong earthquakes, a weak partially infilled masonry wall can act as an auxiliary defense line and form a two-line defense system capable of dissipating more input energy and resisting larger forces.

7. Unlike PISF, in PIOF, the yielding of the beam's longitudinal bars was earlier than the occurrence of diagonal cracks in the infill wall. This implied that the RC frame has acted as the first deference line.

8. Frames with special seismic detailing exhibited a higher deformation capacity when compared with frames with ordinary reinforcement detailing. The calculated displacement ductility ratio (DDR) of SBF was up to 20% larger than OBF and the DDR of PISF was at least 3.5 times more than PIOF.

9. The stiffness degradation rate of partially infilled frames was affected by the failure mechanism of their infill walls. Besides, the partially infilled frames had a faster decay in their normalized stiffness when compared with the bare frames.

10. The cumulative energy dissipation capacity of partially infilled frames calculated at 3% drift ratio was almost 180% more than that of the bare frames. Besides, the employed seismic detailing had an insignificant effect on the energy dissipation of investigated frames.

Author statement

Mahmoud Baniahmadi: Conceptualization, Methodology, Formal analysis, Writing- Original draft preparation. Mohammadreza Vafaei: Funding acquisition, Supervision, Investigation, Validation, Writing - Review & Editing. Sophia C. Alih: Funding acquisition, Supervision, Writing - Review & Editing, Project administration.

Declaration of competing interest

The authors declare that they have no conflict of interests.

Acknowledgments

References

[1] L. Hermanns, A. Fraile, E. Alarcón, R. Álvarez, Performance of buildings with masonry infill walls during the 2011 Lorca earthquake, Bull. Earthq. Eng. 12 (2014) 1977–1997, https://doi.org/10.1007/s10518-013-9499-3.

[2] S.C. Alih, M. Vafaei, Performance of reinforced concrete buildings and wooden structures during the 2015 Mw 6.0 Sabah earthquake in Malaysia, Eng. Fail. Anal. 102 (2019) 351–368, https://doi.org/10.1016/j.engfailanal.2019.04.056.

[3] H. Varum, A. Furtado, H. Rodrigues, J. Dias-Oliveira, N. Vila-Pouca, A. Arêde, Seismic performance of the infill masonry walls and ambient vibration tests after the Ghorka 2015, Nepal earthquake, Bull. Earthq. Eng. 15 (2017) 1185–1212, https://doi.org/10.1007/s10518-016-9999-z.

[4] C.V.R. Murty, S.K. Jain, BENEFICIAL INFLUENCE OF MASONRY INFILL WALLS ON SEISMIC PERFORMANCE OF RC FRAME BUILDINGS, 12 World Conf. Earthq. Eng., Auckland, New Zealand, 2000.

[5] D. Dizhur, J. Ingham, M. Griffith, D. Biggs, A. Schultz, Performance of unreinforced masonry and infilled RC buildings during the 2015 Gorkha, Nepal earthquake sequence. Brick Block Mason Trends, in: Innov Challenges - Proc 16th Int Brick Block Mason Conf IBMAC, 2016, pp. 2399–2408, https://doi.org/10.1201/b21889-314, 2016.

[6] S. Pujol, D. Fick, The test of a full-scale three-story RC structure with masonry infill walls, Eng. Struct. 32 (2010) 3112–3121, https://doi.org/10.1016/j.engstruct.2010.05.030.

[7] M. Di Domenico, P. Ricci, G.M. Verderame, Experimental assessment of the influence of boundary conditions on the out-of-plane response of unreinforced masonry infill walls, J. Earthq. Eng. 24 (2020) 881–919, https://doi.org/10.1080/13632469.2018.1453411.

[8] H. Wijaya, P. Rajeev, E. Gad, A. Amirsardari, Effect of infill-wall material types and modeling techniques on the seismic response of reinforced concrete buildings, Nat. Hazards Rev. 21 (2020), 04020031, https://doi.org/10.1061/(asce)nh.1527-6996.0000395.

[9] M.T. De Risi, M. Di Domenico, P. Ricci, G.M. Verderame, G. Manfredi, Experimental investigation on the influence of the aspect ratio on the in-plane/out-of-plane interaction for masonry infills in RC frames, Eng. Struct. 189 (2019) 523–540, https://doi.org/10.1016/j.engstruct.2019.03.111.

[10] P. Ricci, M. Di Domenico, G.M. Verderame, Experimental investigation of the influence of slenderness ratio and of the in-plane/out-of-plane interaction on the out-of-plane strength of URM infill walls, Construct. Build. Mater. 191 (2018) 507–522, https://doi.org/10.1016/j.conbuildmat.2018.10.011.

[11] F. Di Trapani, G. Macaluso, L. Cavaleri, M. Papia, Masonry infills and RC frames interaction: literature overview and state of the art of macromodeling approach, Eur J Environ Civ Eng 19 (2015) 1059–1095, https://doi.org/10.1080/19648189.2014.996671.

[12] B. Pantò, L. Silva, G. Vasconcelos, P.B. Lourenço, Macro-modelling approach for assessment of out-of-plane behavior of brick masonry infill walls, Eng. Struct. 181 (2019) 529–549, https://doi.org/10.1016/j.engstruct.2018.12.019.

[13] P.G. Asteris, S.T. Antoniou, D.S. Sophianopoulos, C.Z. Chrysostomou, Mathematical macromodeling of infilled frames: state of the art, J. Struct. Eng. 137 (2011) 1508–1517, https://doi.org/10.1061/(asce)st.1943-541x.0000384.

[14] P.G. Asteris, D.M. Cotsovos, C.Z. Chrysostomou, A. Mohebkhah, G.K. Al-Chaar, Mathematical micromodeling of infilled frames: state of the art, Eng. Struct. 56 (2013) 1905–1921, https://doi.org/10.1016/j.engstruct.2013.08.010.

[15] C. Chácara, N. Mendes, P.B. Lourenço, Simulation of shake table tests on out-of-plane masonry buildings. Part (IV): macro and micro FEM based approaches, Int. J. Architect. Herit. 11 (2017) 103–116, https://doi.org/10.1080/15583058.2016.1238972.

[16] A. Furtado, H. Rodrigues, A. Arêde, H. Varum, Experimental tests on strengthening strategies for masonry infill walls: a literature review, Construct. Build. Mater. 263 (2020) 120520, https://doi.org/10.1016/j.conbuildmat.2020.120520.

[17] B. Binici, G. Ozcebe, R. Ozcelik, Analysis and design of FRP composites for seismic retrofit of infill walls in reinforced concrete frames, Compos. B Eng. 38 (2007) 575–583, https://doi.org/10.1016/j.compositesb.2006.08.007.

[18] A. Benavent-Climent, A. Ramírez-Márquez, S. Pujol, Seismic strengthening of low-rise reinforced concrete frame structures with masonry infill walls: shaking-table test, Eng. Struct. 165 (2018) 142–151, https://doi.org/10.1016/j.engstruct.2018.03.026.

[19] E. Yuksel, H. Ozkaynak, O. Buyukozturk, C. Yalcin, A.A. Dindar, M. Surmeli, et al., Performance of alternative CFRP retrofitting schemes used in infilled RC frames, Construct. Build. Mater. 24 (2010) 596–609, https://doi.org/10.1016/j.conbuildmat.2009.09.005.

[20] G. Soltanzadeh, H Bin Osman, M. Vafaei, Y.K. Vahed, Seismic retrofit of masonry wall infilled RC frames through external post-tensioning, Bull. Earthq. Eng. 16 (2018) 1487–1510, https://doi.org/10.1007/s10518-017-0241-4.

[21] C.V.R. Murty, D.C. Rai, S.K. Jain, H.B. Kaushik, G. Mondal, S.R. Dash, Performance of structures in the andaman and nicobar islands (India) during the december 2004 great sumatra earthquake and Indian ocean tsunami, Earthq. Spectra 22 (2006) 321–354, https://doi.org/10.1193/1.2206122.

[22] Ö. Yurdakul, B. Duran, O. Tunaboyu, Ö. Avşar, Field reconnaissance on seismic performance of RC buildings after the January 24, 2020 Elazığ-Sivrice earthquake, Nat. Hazards 105 (2021) 859–887, https://doi.org/10.1007/s11069-020-04340-x.

[23] S.Z. Korkmaz, Observations on the van earthquake and structural failures, J. Perform. Constr. Facil. 29 (2015), 04014033, https://doi.org/10.1061/(asce)cf.1943-5509.0000456.

[24] M. Bruneau, Building damage from the marmara, Turkey earthquake of august 17, 1999, J. Seismol. 6 (2002) 357–377, https://doi.org/10.1023/A:1020035425531.

[25] A. Irfanoglu, Performance of template school buildings during earthquakes in Turkey and Peru, J. Perform. Constr. Facil. 23 (2009) 5–14, https://doi.org/10.1061/(ASCE)0887-3828(2009)23:1(5).

[26] S. Niyompanitpattana, P. Warnitchai, Effects of masonry infill walls with openings on seismic behaviour of long-span GLD RC frames, Mag. Concr. Res. 69 (2017) 1082–1102, https://doi.org/10.1680/jmacr.17.00008.

[27] P.M. Pradhan, R.K. Maskey, P.L. Pradhan, Stiffness behavior and shear effect in partially infilled reinforced concrete frames, J. Earthq. Eng. 18 (2014) 580–588, https://doi.org/10.1080/13632469.2013.873373.

[28] S.W. Han, C.S. Lee, Cyclic behavior of lightly reinforced concrete moment frames with partial- and full-height masonry walls, Earthq. Spectra 36 (2020) 599–628, https://doi.org/10.1177/8755293019899960.

[29] C. Jayaguru, K. Subramanian, Seismic behavior of a partially infilled RC frame retrofitted using GFRP laminates, Exp. Tech. 36 (2012) 82–91, https://doi.org/10.1111/j.1747-1567.2011.00714.x.

[30] J.C. Pineda, Ensayos Experimentales Sobre Control de Columnas Cortas (in Spanish), Proyecto de Grado IC-94-II-26, Advisor: L. E. Garc'a, Departamento, de Ingenierıa Civil, Universidad de los Andes, Bogota, Colombia, 1994, p. 43, n.d.

[31] K.A. Woodward, J.O. Jirsa, Influence of reinforcement on RC short column lateral resistance, J. Struct. Eng. 110 (1984) 90–104, https://doi.org/10.1061/(asce)0733-9445(1984)110:1(90.

[32] K. Maruyama, H. Ramirez, J.O. Jirsa, Short RC columns under bilateral load histories, J. Struct. Eng. 110 (1984) 120–137, https://doi.org/10.1061/(asce)0733-9445(1984)110:1(120).

[33] Q. Huang, Z. Guo, J.S. Kuang, Designing infilled reinforced concrete frames with the "strong frame-weak infill" principle, Eng. Struct. 123 (2016) 341–353, https://doi.org/10.1016/j.engstruct.2016.05.024.

[34] A.D. Dautaj, Q. Kadiri, N. Kabashi, Experimental study on the contribution of masonry infill in the behavior of RC frame under seismic loading, Eng. Struct. 165 (2018) 27–37, https://doi.org/10.1016/j.engstruct.2018.03.013.

[35] J. Zovkic, V. Sigmund, I. Guljas, Cyclic testing of a single bay reinforced concrete frames with various types of masonry infill, Earthq. Eng. Struct. Dynam. 42 (2013) 1131–1149, https://doi.org/10.1002/eqe.2263.

[36] L.T. Guevara, L.E. García, The captive- and short-column effects, Earthq. Spectra 21 (2005) 141–160, https://doi.org/10.1193/1.1856533.

[37] M. Vafaei, M. Baniahmadi, S.C. Alih, The relative importance of strong column-weak beam design concept in the single-story RC frames, Eng. Struct. 185 (2019) 159–170, https://doi.org/10.1016/J.ENGSTRUCT.2019.01.126.

[38] MI, ACI 318, Building Code Requirements for Structural Concrete (ACI 318–14) and Commentary on Building Code Requirements for Structural Concrete (ACI 318R-14), American Concrete Institute, Farmington Hills, 2014.

[39] BS EN 1998-1, Eurocode 8, Design of Structures for Earthquake Resistance. Part 1.3: General Rules-specific Rules for Various Materials and Elements, Commission of the European Communities. n.d, Brussels, 2004.

[40] ASTM C1314 - 18 Standard Test Method for Compressive Strength of Masonry Prisms, American Society for Testing and Materials,. 2018.

[41] ASTM E519/E519M - 15 Standard Test Method for Diagonal Tension (Shear) in Masonry Assemblages, American Society for Testing and Materials. 2015.

[42] FEMA 461, Interim Testing Protocols for Structural and Nonstructural Performance Characteristics of Determining the Seismic Components, Redwood City, California, 2007.

[43] ASCE/SEI 41-17, Seismic Rehabilitation and Retrofit of Existing Buildings, American Society of Civil Engineers (ASCE), Reston, Virginia, 2017.

[44] U.A. Siddiqui, H. Sucuoğlu, A. Yakut, Seismic performance of gravity-load designed concrete frames infilled with low-strength masonry, Earthq Struct 8 (2015) 19–35, https://doi.org/10.12989/eas.2015.8.1.019.

[45] W M, H M, Failure OF shear-stressed masonry: an enlarged theory, tests and application to shear walls, Proc. Br. Ceram. Soc. ISSN (1982) 223–235, 0524-5141; GBR; DA. 1982; NO 30.

[46] F.J. Crisafulli, A.J. Carr, R. Park, Analytical modelling of infilled frame structures - a general review, Bull New Zeal Soc. Earthq. Eng. 33 (2000) 30–47, https://doi.org/10.5459/bnzsee.33.1.30-47.

[47] F.J. Crisafulli, A.J. Carr, Proposed macro-model for the analysis of infilled frame structures, Bull New Zeal Soc. Earthq. Eng. 40 (2007) 69–77, https://doi.org/10.5459/bnzsee.40.2.69-77.

[48] American Society of Civil Engineers (ASCE), FEMA 356 Prestandard and Commentary for the Seismic Rehabilitation of Building, 2000. Reston, Virginia.